
Research Paper

The Use of Amino Acid Linkers in the Conjugation of Paclitaxel with Hyaluronic Acid as Drug Delivery System: Synthesis, Self-Assembled Property, Drug Release, and *In Vitro* Efficiency

Dingcheng Xin,^{1,2} Ying Wang,^{1,2,3} and Jiannan Xiang^{1,2,3,4}

Received April 22, 2009; accepted October 15, 2009; published online October 30, 2009

Purpose. A cell-targeted prodrug with good self-assembly properties in aqueous solution was prepared for the anti-cancer drug paclitaxel, offering great potential for further investigation.

Methods. We synthesized hyaluronic acid (HA) with a specific targeting property as a carrier to conjugate with paclitaxel by inserting different amino acids as spacers, including valine, leucine, and phenylalanine, respectively. The structure of HA-amino acid-paclitaxel conjugates was characterized by ¹H NMR and GPC. The loading weight and hydrolysis rate were detected by UV and HPLC, respectively. Their morphology and mean diameter were investigated by SEM and DLS, respectively. The biological activity of HA-amino acid-paclitaxel conjugates was measured by MTT assay and flow cytometry using MCF-7 cells.

Results. The use of amino acids as spacers between drug and carrier facilitated paclitaxel release from the conjugates. Their morphology demonstrated that the prepared prodrugs could self-assemble to form nanoparticles with a narrow size distribution and spherical shape. Furthermore, the prodrugs exhibited increased cytotoxicity as compared to free drug. Flow cytometry analysis showed that MCF-7 cells treated with conjugates were arrested in the G₂/M phase of the cell cycle.

Conclusions. Prodrugs synthesized as HA-amino acid-paclitaxel conjugates exhibited enhanced cytotoxicity in breast cancer cell lines and hence may have potential application as tumor-specific nanoparticulate therapeutic agents.

KEY WORDS: amino acid; hyaluronic acid; synthesis; self-assembled property.

INTRODUCTION

Paclitaxel is a powerful anticancer drug originally isolated from the bark of *Taxus brevifolia* (*Pacific yew*) and is a well-known antitumor agent adopted mainly for the treatment of breast and ovarian cancer (1). Paclitaxel is a mitotic inhibitor which acts by interfering with the depolymerization of microtubules during cell division and inhibits cell replication in the late G₂/M phase of the cell cycle (2,3). However, its poor solubility in water has limited its use in cancer therapy. It is generally administered as a castor oil (Cremophor®) / EtOH solution which

usually brings toxic side-effects, such as hypersensitivity, neurotoxicity, and nephrotoxicity (4,5).

In recent years, macromolecules for the targeted delivery of anticancer agents have generated considerable interest due to their enhanced permeability and retention (EPR) effect in tumor tissues (6–8). Extensive research in this area has included formulating paclitaxel in various carriers, such as polymer conjugates, liposomes, polymeric micelles, emulsions, nanospheres and others (9–12). Synthesis of drug-polymer conjugates with self-assembly properties brings distinct advantages over conventional polymeric carrier drug delivery systems by demonstrating good solubility in water and enhanced antitumor effects (10,13). The pharmaceutical activity of self-assembled nanoscale drug delivery systems has recently attracted considerable attention (14–16). It was reported that a three-dimensional network of nanofibers formed by self-assembly of peptide-amphiphiles could become a possible approach for controlled release of growth factors and were applied in drug delivery and tissue engineering (17–21). Generally, self-assembled nanoparticles for drug delivery systems, such as amphiphilic block copolymer micelles, have a hydrophobic inner core and a hydrophilic outer shell, and subsequently various hydrophobic anticancer drugs have been physically entrapped within the core of copolymers. The nanoscale drug delivery system can increase

Dingcheng Xin and Ying Wang have equal contribution in this work and are both equally considered as first author.

¹ Biomedical Engineering Center, Hunan University, Changsha, Hunan 410082, People's Republic of China.

² College of Chemistry and Chemical Engineering, Hunan University, Changsha, Hunan 410082, People's Republic of China.

³ State Key Laboratory of Chemo/Biosensing and Chemometrics, Hunan University, Changsha, Hunan 410082, People's Republic of China.

⁴ To whom correspondence should be addressed. (e-mail: jnxiang@hnu.cn)

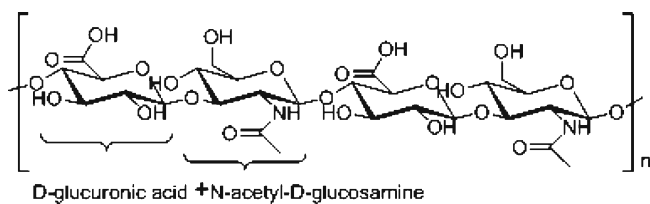


Fig. 1. Structure of hyaluronic acid.

the parent drug solubility as well as maintain the structural integrity of the drug, which can have applications for enhancing paclitaxel solubility.

Hyaluronic acid (HA) (Fig. 1) is a linear polysaccharide, containing two alternating units of **D**-glucuronic acid (GlcUA) and **N**-acetyl-**D**-glucosamine (GlcNAc). It can be found throughout connective, epithelial and neural tissues. HA plays important roles in biological functions, such as cell adhesion, growth, and migration (22). HA also acts as a signaling molecule in cell motility, inflammation, wound healing, and cancer metastasis (23). It has a strong affinity to cell-specific surface markers, such as glycoprotein CD44 and receptor for hyaluronic acid-mediated motility (RHAMM), which are overexpressed on the surface of many types of tumors (24–26). The biocompatibility, biodegradability, and specific targeting property of HA make it an ideal drug delivery vehicle for various therapeutic agents, such as butyric acid and doxorubicin (27–30). Prestwich and co-workers reported a HA-paclitaxel conjugate using adipic dihydrazide as a linker (31,32). It was shown that this HA-paclitaxel conjugate was internalized into cancer cells through receptor-mediated endocytosis, followed by intracellular

release of active drug while maintaining paclitaxel's original cytotoxicity. However, *in vitro* drug release experiments show that this HA-paclitaxel conjugate is quite long-lived, with less than 20% of paclitaxel released from the conjugate in cell culture media within 24 h.

Our previous research demonstrates that compared to the direct ester bond between carrier and drug, conjugates with different amino acids as linkers progressively liberate much more paclitaxel in physiological and enzymatic conditions (33). Accordingly, we selected amino acids as spacer between paclitaxel and carrier instead of a direct ester bond. Therefore, in this study we developed HA-paclitaxel conjugates using amino acids as linkers, including valine, leucine, and phenylalanine. Meanwhile, we investigated the behavior of HA-amino acid-paclitaxel in aqueous solution and examined whether conjugation of paclitaxel to HA by the different amino acid spacers would influence the pharmaceutical activity as compared with native paclitaxel. In addition, the *in vitro* cytotoxicity and effect on cell cycle progression of prodrugs were evaluated in the MCF-7 human breast-cancer cell line using free paclitaxel as a control.

MATERIALS AND METHODS

Materials

Hyaluronic acid (sodium salt, $M_n=9.8$ kDa) was purchased from Shandong Freda Biochem Co., Ltd. (Shandong, China). 732 (H^+) cation-exchange resin was obtained from Shanpu Co., Ltd. (Shanghai, China). Tetrabutylammonium

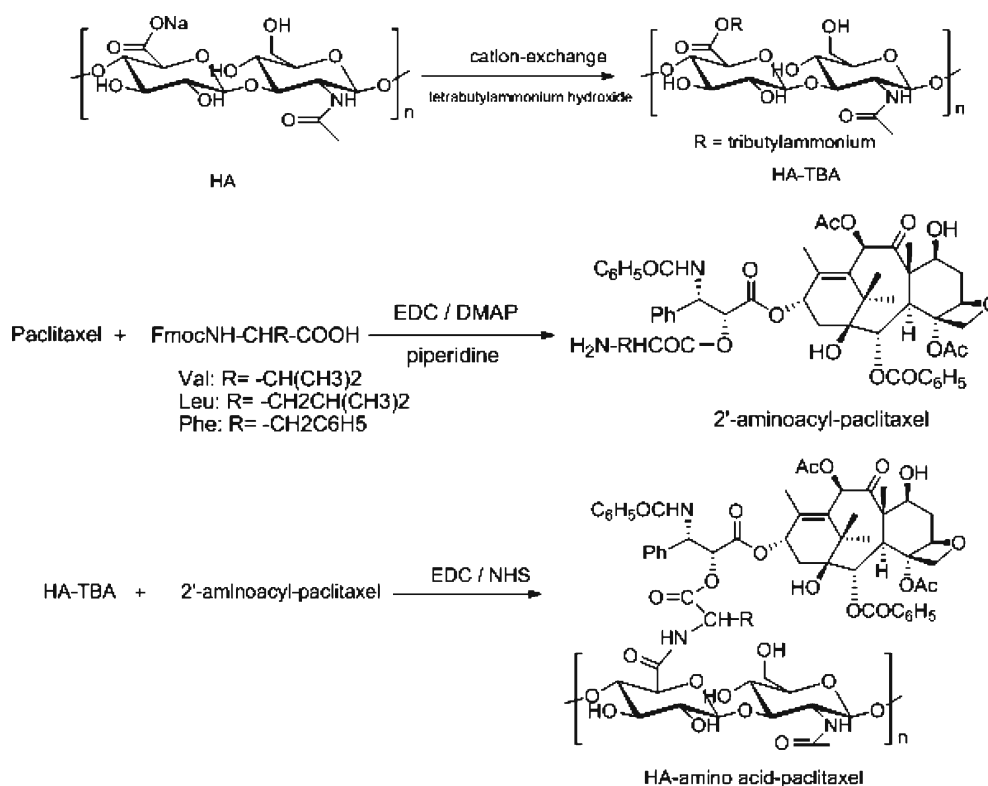


Fig. 2. Synthesis of HA-amino acid-paclitaxel.

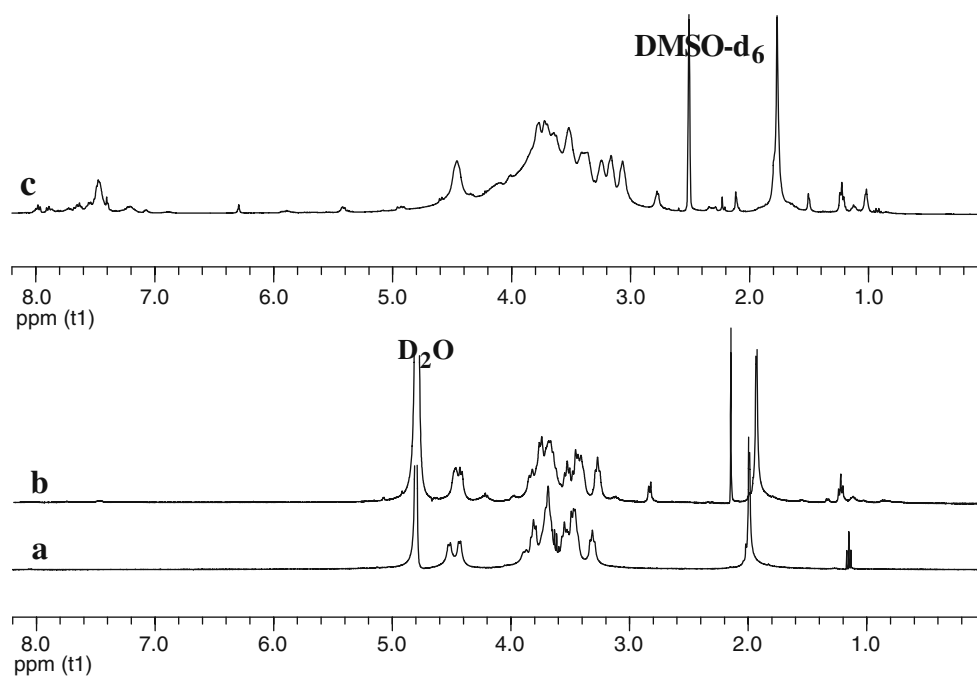


Fig. 3. ^1H NMR spectra of **a** HA in D_2O , **b** HA-pheylalanyl-paclitaxel in D_2O and **c** HA-pheylalanyl-paclitaxel in $\text{DMSO-}d_6$.

hydroxide and N, N'-dimethylformamide (DMF) were purchased from Sinopharm chemical reagent Co., Ltd. (Shanghai, China), and paclitaxel (Taxol®) came from Tecano Science & Technology Co., Ltd. (Guangzhou, China). 2'-Valyl-paclitaxel, 2'-Leucyl-paclitaxel, and 2'-Pheylalanyl-paclitaxel were prepared in our lab. 1-Ethyl-3-(3-dimethylaminopropyl) carbodiimide hydrochloride (EDC), N-Hydroxysuccinimide (NHS) were obtained from Shanghai medpep Co., Ltd. (Shanghai, China). Dialysis membrane (MWCO 3,500) was purchased from Viskase Co., Inc. (Illinois, USA). Reaction solvents were purified by distillation under nitrogen prior to use. Hyaluronidase was

purchased from Sigma-Aldrich Co., Inc. (USA). Ultrapure water (Milli-Q, 18.2 M Ω) was used in the experiment. MCF-7 (breast carcinoma) cell line was provided by the Institute of Life Science and Biotechnology in Hunan University.

Synthesis of HA-Amino Acid-Paclitaxel

The HA-amino acid-paclitaxel compounds were prepared as shown in Fig. 2. Hyaluronic acid sodium salt was first converted to the corresponding tetrabutylammonium salt (HA-TBA), which has good solubility in polar aprotic organic solvents (34). Hyaluronic acid sodium salt (0.5 g) was dissolved in 10 mL of water and then percolated through a column (200 mL) of 732 (H^+) cation-exchange resin at 4°C. The pH of the solution was adjusted to 6.0 by addition of tetrabutylammonium hydroxide (3 mL). Excess tetrabutylammonium hydroxide was dialyzed against deionized water using dialysis membrane for 3 days. Water was eliminated upon evaporating and a concentrated HA-TBA solution was obtained. After lyophilizing, HA-TBA (0.75 g) was obtained. 2'-

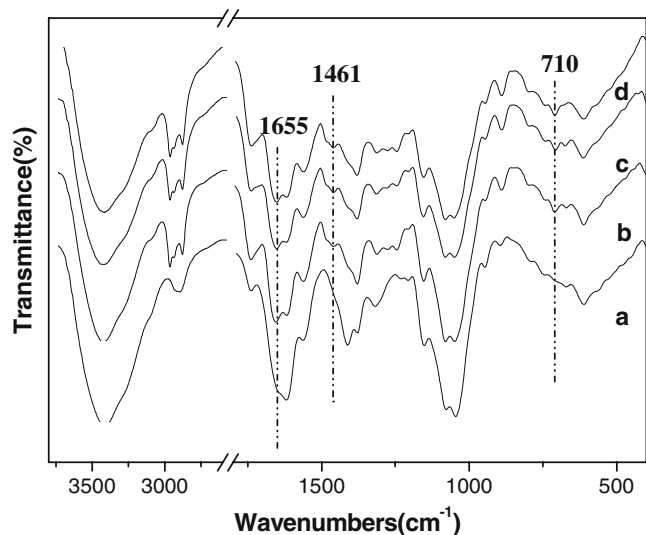


Fig. 4. IR spectra of **a** HA, **b** HA-valyl-paclitaxel, **c** HA-leucyl-paclitaxel and **d** HA-pheylalanyl-paclitaxel.

Table I. M_n , Polydispersity Index (PDI) and Percentage Weight of Drug for HA-Amino Acid-Paclitaxel Conjugates by GPC and UV Measurements

Conjugate	M_n	Polydispersity index (PDI)	Paclitaxel loading amount (w/w %)
HA-valyl-paclitaxel	11,660	1.95	10.8
HA-leucyl-paclitaxel	11,807	2.14	12.1
HA-pheylalanyl-paclitaxel	12,173	2.34	14.5

Valyl-paclitaxel (50 mg, 0.055 mmol) and HA-TBA (250 mg) were dissolved in dry DMF (15 mL) containing EDC (28 mg, 0.15 mmol) and NHS (18 mg, 0.15 mmol), and the reaction mixture was stirred at 35°C. After 24 h, the final product was purified by dialyzing against deionized water for 3 days to remove residual solvents. After lyophilization, HA-valyl-paclitaxel (230 mg) was obtained as a white powder. HA-leucyl-paclitaxel and HA-phenylalanyl-paclitaxel were synthesized as described for the method of HA-valyl-paclitaxel.

Preparation of Self-Assembled Nanoparticles

The HA-amino acid-paclitaxel conjugates were dissolved in distilled water at 25°C, and each solution was sonicated for 20 s. In this way, HA-amino acid-paclitaxel conjugates formed self-assembled nanoparticles in aqueous solution.

Characterization of HA-Amino Acid-Paclitaxel

The ¹H NMR spectral data were obtained using a Varian INOVA400 apparatus. FT-IR spectra were determined by a FD-5DX infrared spectrum apparatus. UV spectra were recorded on a UV-2300 Spectrophotometer (Techcomp, China). The percentage weight of drug on the conjugates was estimated by UV measurement based on a standard curve generated with known concentrations of paclitaxel in ethanol ($\lambda=228$ nm). Gel permeation chromatography (GPC)

was carried out on a Waters 515 GPC system (Waters, USA) equipped with a Waters Ultrahydrogel 250 Column, using a Waters 410 refractive index detector. 0.1 mol/L NaCl was used as an elution solvent at a flow rate of 0.6 mL/min, and the column temperature was maintained at 40°C using polyethylene glycol standards.

Characterization of Self-Assembled Nanoparticles

Size distribution and zeta potential of conjugates were measured at 25°C using a Zetasizer Nano-Zs (Malvern Instruments, UK). The concentration of self-aggregates was kept constant at 0.3 mg/mL. The morphology of nanoparticles was observed on a scanning electron microscope (SEM), which was performed on a JSM-6700F scanning electron microscope (JEOL, Japan). The conjugates in distilled water were mounted on a metal stub and left to dry. The dried samples were coated with a gold layer using a SCD-050 sputter coater (BAL-TEC, Liechtenstein) at 10^{-2} mbar and 15 mA for 50 s, and viewed by SEM at a voltage of 5.0 kV.

In Vitro Release of Paclitaxel from HA-Amino Acid-Paclitaxel Conjugates

HA-amino acid-paclitaxel conjugates were dissolved in phosphate-buffered saline (PBS, 0.01 M) at pH 7.4 or pH 5.0

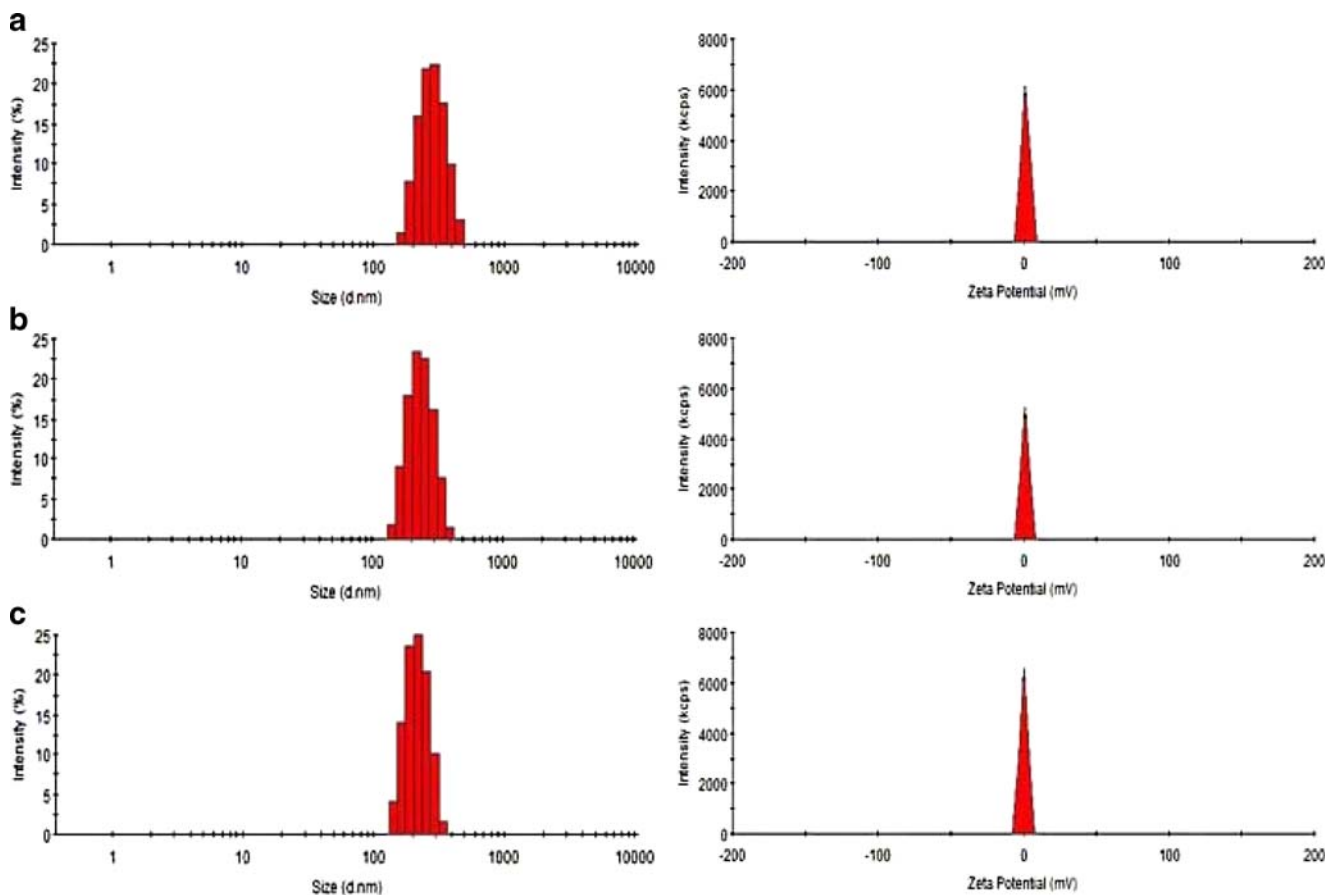


Fig. 5. Size distribution and zeta potential of **a** HA-valyl-paclitaxel, **b** HA-leucyl-paclitaxel, and **c** HA-phenylalanyl-paclitaxel by DLS analysis in aqueous solution.

and hyaluronidase (10 U/mL) in PBS (0.01 M) at pH 7.4 or pH 5.0 at an equivalent paclitaxel concentration of 1 g/L. The solutions were incubated at 37°C with gentle shaking at 50 rpm. At selected time intervals, aliquots (500 μ L) were removed, and an equivalent PBS concentration was added to the solutions. The aliquots were extracted by chloroform, and the organic fraction was evaporated. Residue was mixed with acetonitrile (1,000 μ L) and analyzed using HPLC.

HPLC was carried out on a Shimadzu LC-20AT system (Shimadzu, Japan) consisting of a SepaxHP-C18 reverse-phase silica column (Sepax, USA), a mobile phase of acetonitrile and 0.05% trifluoroacetic acid in water (60:40) pumped at a flow rate of 1.0 mL/min. The column effluent was detected at 227 nm with a SPD-20A UV detector (Shimadzu, Japan).

In Vitro Cell Culture Cytotoxicity

MCF-7 cells were seeded in 96-wells plates (5,000 cells/well) in RPMI-1640 medium supplemented with 10% fetal calf serum. The cells were allowed to adhere for 24 h at 37°C, and the seeding medium was removed and replaced with experimental medium. The cytotoxicity of HA-amino acid-paclitaxel conjugates was determined with increasing doses: 0.01, 0.1, 1, 10, and 100 μ g/mL (concentration of paclitaxel equivalent). The experiment was performed at least thrice, and samples were run in eight replicates. Cells were incubated at 37°C for 2 days with the test material. Cell viability in cell culture was determined by thiazoyl blue (MTT) dye with absorbance measured at

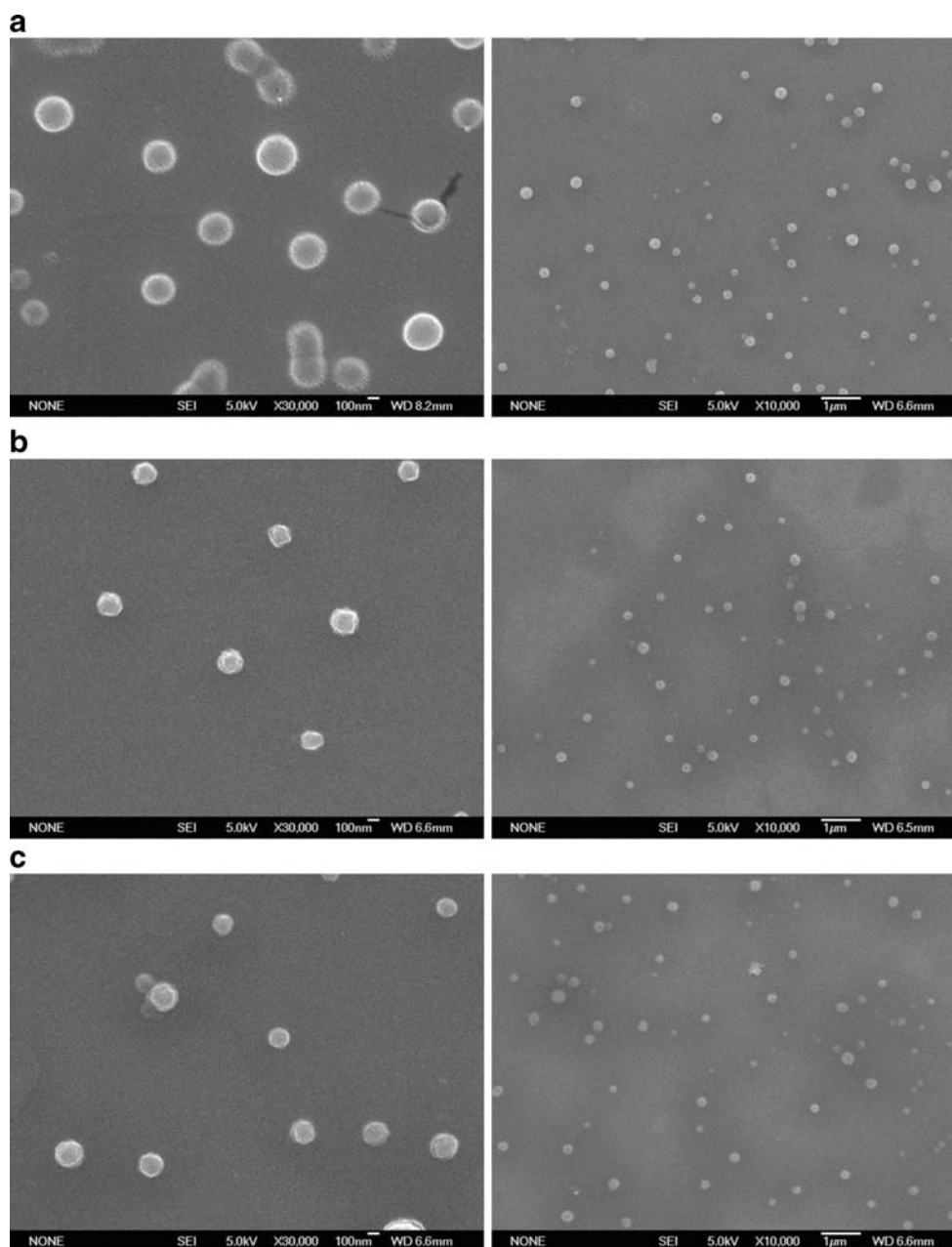


Fig. 6. Scanning electron microscopy photographs of **a** HA-valyl-paclitaxel (magnification: $\times 30,000$, $\times 10,000$); **b** HA-leucyl-paclitaxel (magnification: $\times 30,000$, $\times 10,000$); **c** HA-phenylalanyl-paclitaxel (magnification: $\times 30,000$, $\times 10,000$).

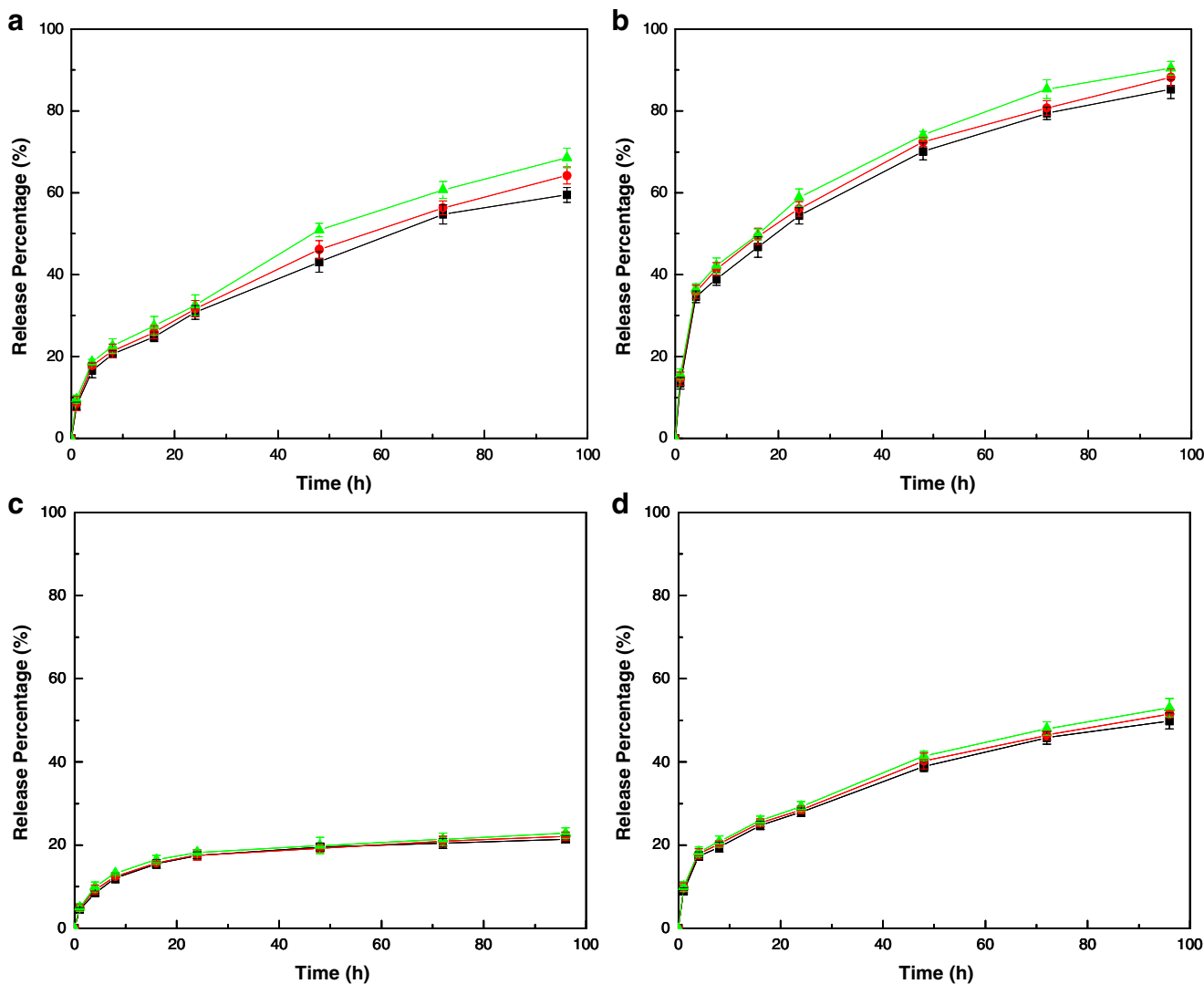


Fig. 7. *In vitro* release profiles of paclitaxel from HA-valyl-paclitaxel (■), HA-leucyl-paclitaxel (●) and HA-phenylalanyl-paclitaxel (▲) under various conditions. **a** in pH 7.4 PBS, **b** with hyaluronidase in pH 7.4 PBS, **c** in pH 5.0 PBS, **d** with hyaluronidase in pH 5.0 PBS. The data represent mean \pm S.D. where $n=3$.

570 nm, which was recorded on a Multiskan MK3 microplate reader (Thermo, USA).

Flow Cytometric (FCM) Assay

Cell cycle analyses were performed on EPICS-XL flow cytometer (Beckman Coulter, USA), and data were analyzed by Mcycle software. MCF-7 cells were seeded on a 6-well plate and preincubated for 24 h, followed by coincubation with paclitaxel and HA-amino acid-paclitaxel conjugates (an

equivalent paclitaxel concentration of 100 $\mu\text{g/mL}$) for 6 h. The cells were then washed three times with PBS, detached by trypsinizatin, spun down by centrifugation, and dispersed again in PBS for flow cytometry analysis.

Statistical Analysis

The data were represented as the means \pm standard deviation (S.D.). Statistical comparisons ($n=3$) were performed with student’s t-test.

Table II. *In Vitro* Release Rate of Paclitaxel from HA-Amino Acid-Paclitaxel

Conjugate	$t_{1/2}$ (h)			
	PBS (pH 7.4)	PBS (pH 7.4) with hyaluronidase	PBS (pH 5.0)	PBS (pH 5.0) with hyaluronidase
HA-valyl-paclitaxel	63	19	ND ^a	96
HA-leucyl-paclitaxel	57.5	17	ND	89
HA-phenylalanyl-paclitaxel	47	16	ND	81.5

^a ND not detected

RESULTS AND DISCUSSION

It was reported that the instability of the 2'-glycyl ester salt was probably due to a simple inductive effect of the protonated amino group assisting in the attack of external nucleophiles on the 2'-acyl group (35). Therefore, amino acids with different α -substituted group, such as isopropyl, isobutyl, and benzyl, were selected to increase the stability. In this study, we first synthesized 2'-aminoacyl paclitaxel, including 2'-Valyl-Paclitaxel, 2'-Leucyl-Paclitaxel, 2'-Pheylalanyl-Paclitaxel, and then they were introduced to the carrier. Since amino acids have bi-functional groups, they provided a reactive carboxyl group conjugated with paclitaxel and an amino group with HA.

Characterization of HA-Amino Acid-Paclitaxel

^1H NMR spectra of HA and HA-pheylalanyl-paclitaxel was shown in Fig. 3. It was measured in two different solvents (D_2O and $\text{DMSO-}d_6$). Compared with that of HA, the conformation of HA-amino acid-paclitaxel made some difference in ^1H NMR due to paclitaxel introduced to the carrier. The signals of the methyl of the O-acetyl group were shifted to 1.7~1.9 ppm, and glucosidic protons were attributed to 3.0~5.0 ppm in D_2O and $\text{DMSO-}d_6$. But specific glucosidic protons were difficultly identified in D_2O and $\text{DMSO-}d_6$ due to conformational change.

Due to the hydrophobic property of paclitaxel, a majority of paclitaxel signals in HA-pheylalanyl-paclitaxel in $\text{DMSO-}d_6$ were observed. The partial signals of paclitaxel in high field can be slightly detected in D_2O , a benzene ring at 7.0~8.0 ppm in low field was hardly observed. It might be good water-solubility of HA resulting in amphiphilic properties of HA-amino acid-paclitaxel. These results showed amphiphilic character of the prepared prodrugs. HA-amino acid-paclitaxel conjugates self-assembled to form nanoparticles in aqueous solution, which were likely to have a core/shell structure composed of a hydrophobic inner core containing aggregated paclitaxel molecules and a hydrophilic HA shell layer.

The NMR results confirm the formation of HA-amino acid-paclitaxel, which is further supported by the FT-IR spectra. Fig. 4 showed the IR spectra of HA and HA-amino acid-paclitaxel. A new band at $1,655\text{ cm}^{-1}$ was assigned to the ester bond vibration in spectra b, c and d (36). After paclitaxel introduced to the carrier, the band at $1,461\text{ cm}^{-1}$, 710 cm^{-1} appeared in spectra b, c and d, which were attributed to the $-\text{C}=\text{C}-$ stretching mode of benzene ring of paclitaxel, which indicated that paclitaxel was successfully linked to the carrier, forming HA-amino acid-paclitaxel.

GPC measurement in aqueous phase showed the average molecular weight (M_n) and polydispersity index (PDI) of HA-amino acid-paclitaxel conjugates (Table I). The loading weight of drug was quantified by UV absorbance ($\lambda = 228\text{ nm}$), assuming that the conjugates in water and the free drug in ethanol had the same molar extinction coefficients and that both followed Lambert Beer's law (37). The calculated weight of HA-amino acid-paclitaxel conjugates contained 10~15% paclitaxel (w/w) corresponding to the results of GPC.

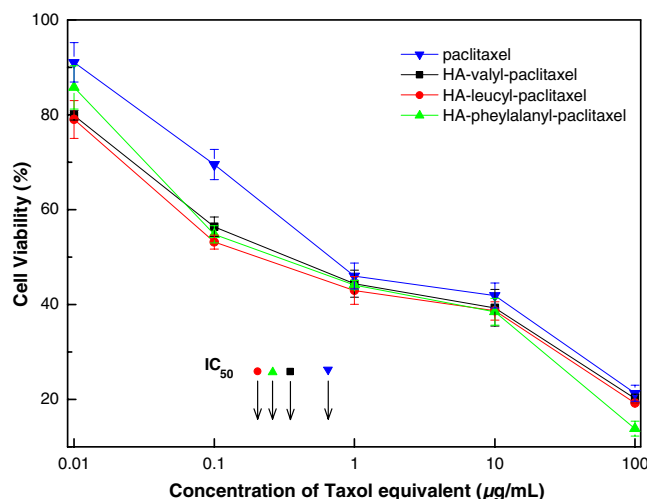


Fig. 8. *In vitro* cytotoxicity of HA-amino acid-paclitaxel conjugates against MCF-7 cells. The data represent mean \pm S.D. where $n=3$.

Characterization of Self-Assembled Nanoparticles

It is reported that amphiphilic copolymers can self-assemble to form nanoparticles in aqueous solution via hydrophobic interactions (38). Due to the amphiphilic characteristics of HA-amino acid-paclitaxel conjugates composed of hydrophilic HA and hydrophobic paclitaxel, we investigated their self-assembled behavior in aqueous solution. The particle size and zeta potential were measured by DLS (Fig. 5), and the average diameter of HA-valyl-paclitaxel, HA-leucyl-paclitaxel and HA-pheylalanyl-paclitaxel was $282 \pm 8\text{ nm}$, $285 \pm 13\text{ nm}$, $275 \pm 11\text{ nm}$, respectively. The surface charge of nanoparticles was found to be an important factor contributing to the efficiency of drug delivery, and cell surface charge interactions with the external materials affected cellular uptake. (39–43). HA-amino acid-paclitaxel conjugates exhibited the zeta potential of an almost zero charge, which was $+0.43\text{ mV}$, $+0.23\text{ mV}$ and $+0.17\text{ mV}$, respectively. The results suggested that aminoacyl paclitaxel reacted with the carboxyl groups of HA to form nanoparticles with a neutral surface. It was possible to make the slightly positively charged nanoparticles internalize into cells after

Table III. *In Vitro* Cytotoxicity of HA-Amino Acid-Paclitaxel Conjugates Against MCF-7 Cells

Compound	IC_{50}	
	$\mu\text{g/mL}$ (compound) ^a	nM (paclitaxel equivalent) ^b
Paclitaxel	0.68	0.795
HA-valyl-paclitaxel	3.19	0.406
HA-leucyl-paclitaxel	1.77	0.253
HA-pheylalanyl-paclitaxel	1.97	0.336

This calculation allows comparison of compound and free drug.

^a The data show IC_{50} of HA-amino acid-paclitaxel against MCF-7.

^b The data are calculated as the paclitaxel equivalents present in the HA-amino acid-paclitaxel using the molar ratios.

the attachment onto the negatively charged cell membrane. This would result in enhancement of drug delivery. The SEM images were obtained to visualize HA-amino acid-paclitaxel conjugate nanoparticles. In Fig. 6, round-shaped nanoparticles were observed with diameter 260~270 nm, corresponding well to the size measured by DLS. HA-amino acid-paclitaxel conjugate nanoparticles were likely to have a core/shell structure composed of a hydrophobic inner core containing aggregated paclitaxel molecules and a hydrophilic HA shell layer. Also, SEM showed that nanoparticles were well-dispersed with spherical shape.

In Vitro Release of Paclitaxel from HA-Amino Acid-Paclitaxel Conjugates

In this study, conjugates were exposed to chemical and enzymatic conditions to test the drug release at pH 7.4 and pH 5.0. The results of the release rates are reported in Fig. 7 and Table II. It was shown that without enzyme, over 45% (w/w) of paclitaxel was released from conjugates after 48 h at pH 7.4, while about 19% (w/w) of paclitaxel was liberated at pH 5.0. Meanwhile, a drug release half-life ($t_{1/2}$) of HA-leucyl-paclitaxel was 60 h at pH 7.4, which was similar to that of HA-valyl-paclitaxel. In addition, HA-phenylalanyl-paclitaxel showed a faster rate ($t_{1/2}$ =48 h) at pH 7.4. Compared to the above condition without enzyme, the release rate of paclitaxel increased sharply in the presence of hyaluronidase. Over 55% (w/w) of paclitaxel was released

from conjugates after 24 h at pH 7.4 with hyaluronidase and hydrolysis rates of HA-amino acid-paclitaxel conjugates showing a faster growth trend ($t_{1/2}$ ≈17 h). About 40% (w/w) of paclitaxel was liberated after 48 h at pH 5.0 with hyaluronidase. As a whole, the hydrolysis rates of conjugates at pH 7.4 were faster than that of conjugates at pH 5.0. Under enzymatic conditions, much more paclitaxel was released from conjugates.

Nicolaou (44) and co-workers synthesized a series of paclitaxel prodrugs and demonstrated that strong electron withdrawing substituent in the α -position of the paclitaxel ester may accelerate the hydrolytic cleavage of paclitaxel. Our previous work showed that direct ester bond between carrier and drug was difficult to hydrolyze. Therefore, we selected amino acids as spacer between paclitaxel and carrier instead of a direct ester bond. Meanwhile, these results are consistent with our previous findings (33). It was reported by Prestwich and co-workers that HA-paclitaxel conjugate using adipic dihydrazide as a linker released less than 20% of paclitaxel in cell culture media within 24 h. It was found that the drug was liberated from HA-paclitaxel conjugate by direct ester bond hydrolysis (31). Due to the electron effect of the protonated amino group, HA-amino acid-paclitaxel conjugates showed higher drug release rates under both the pH 7.4 condition and the pH 7.4 with hyaluronidase condition. This suggested that the molecular design of amino acids as linker facilitated the release of paclitaxel from HA.

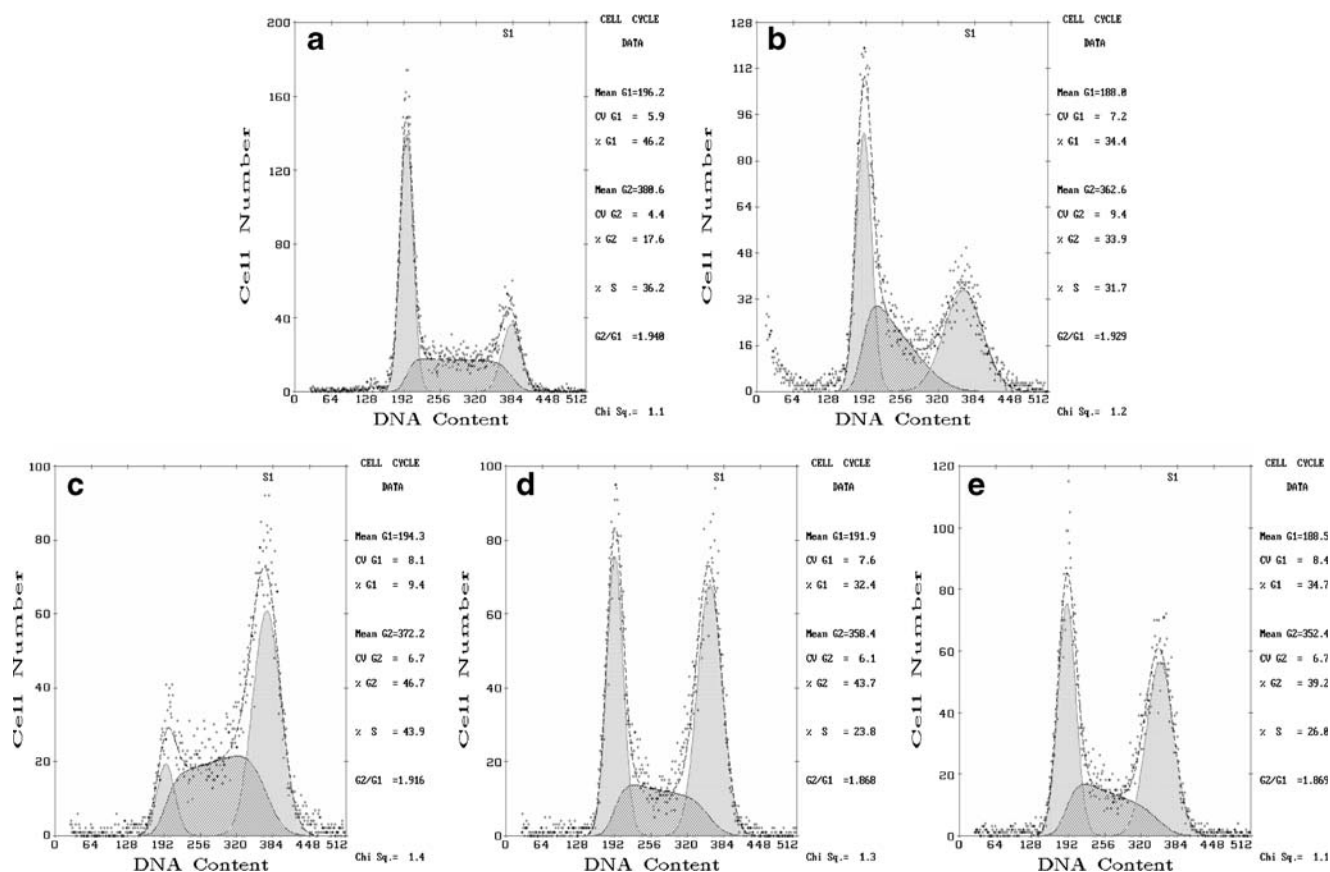


Fig. 9. Flow cytometric analysis of the cell cycle profiles of MCF-7 cells treated with paclitaxel and HA-amino acid-paclitaxel conjugate for 6 h. a control cells, b paclitaxel, c HA-valyl-paclitaxel, d HA-leucyl-paclitaxel, e HA-phenylalanyl-paclitaxel.

In Vitro Toxicity and Cell Cycle Analysis

Fig. 8 shows the cytotoxicity for HA-amino acid-paclitaxel conjugates. As compared to free paclitaxel, HA-amino acid-paclitaxel conjugates showed more cytotoxicity against MCF-7 cells (Table III). Among the three kinds of conjugates, HA-leucyl-paclitaxel was more effective than any other conjugate. It exhibited a lower IC₅₀ value (0.253 nM paclitaxel equivalent) and was roughly 3 fold lower than that of free paclitaxel (0.795 nM). The extent of apoptosis was quantitatively assessed by flow cytometry analysis. Since the cytotoxic activity of paclitaxel is mainly due to its stabilizing effect on polymerized microtubules necessary for spindle formation and cell division, paclitaxel has been shown to cause a cell cycle arrest in the G₂/M phase and finally cell death through an apoptotic mechanism (45,46). Fig. 9 shows the cell cycle profile of MCF-7 treated with paclitaxel and HA-amino acid-paclitaxel conjugates. As compared with control cells, the sharp peak observed in the G₀/G₁ phase was markedly attenuated and was decreased instead of the peak for the G₂/M phase for cells treated with paclitaxel and HA-amino acid-paclitaxel conjugates. HA-amino acid-paclitaxel conjugate nanoparticles induced a significant increase in G₂/M cell population (46.7%, 43.7% and 39.2%, respectively), compared to that of paclitaxel (33.9%). Consequently, these results demonstrated that conjugate nanoparticles significantly enhanced the extent of apoptosis-induced cell death. Nanosized and self-assembled HA-amino acid-paclitaxel conjugate nanoparticles could be utilized as efficient all-in-one carriers not only for the solubilization of paclitaxel, but also for its passive and active targeted delivery to cancer cells.

CONCLUSION

We designed and synthesized a class of novel drug delivery systems using amino acids as the linker between HA and paclitaxel, which showed shorter half-lives ($t_{1/2}$) under physiological and enzymatic conditions. Specifically, the as-prepared prodrug could self-assemble nanoparticles, which could increase the parent drug solubility as well as maintain the structural integrity of drug. In *in vitro* experiments, nanosized prodrugs exhibited increased cytotoxicity as compared to free drug paclitaxel against the MCF-7 human breast-cancer cell line. Cell cycle analysis studied by flow cytometry showed that conjugates could block MCF-7 cells at the G₂/M phase. Taken together, HA-amino acid-paclitaxel conjugate offered promising potential for further investigation. The *in vivo* research about the HA-amino acid-paclitaxel drug delivery system is underway in our lab.

ACKNOWLEDGEMENT

The authors are grateful for the financial support of 985 Foundation of Ministry of Education. This work was supported by the National Natural Science Foundation of China (Grant No. 20472018), by the Natural Science Foundation of Hunan (Key Project No. 07JJ3019), by the Department of Science and Technology of Changsha (Grant No. K082152).

REFERENCES

1. Wani MC, Taylor HL, Wall ME, Coggon P, McPhail AT. Plant antitumor agents. VI. The isolation and structure of taxol, a novel antileukemic and antitumor agent from *Taxus brevifolia*. *J Am Chem Soc.* 1971;93:2325-7.
2. Schiff PB, Fant J, Horwitz SB. Promotion of microtubule assembly *in vitro* by taxol. *Nature.* 1979;277:665-7.
3. Rowinsky EK, Donehower RC, Jones RJ, Tucker RW. Microtubule changes and cytotoxicity in leukemic cell lines treated with taxol. *Cancer Res.* 1988;48:4093-100.
4. Weiss RB, Donehower RC, Wiernik PH, Ohnuma T, Gralla RJ, Trump DL, *et al.* Hypersensitivity reactions from taxol. *J Clin Oncol.* 1990;8:1263-8.
5. Singla AK, Garg A, Aggarwal D. Paclitaxel and its formulations. *Int J Pharm.* 2002;235:179-92.
6. Francesco MV, Oddone S, Gianfranco P, Raniero M, Ruth D. PEG-doxorubicin conjugates: influence of polymer structure on drug release, *in vitro* cytotoxicity, biodistribution, and antitumor activity. *Bioconjugate Chem.* 2005;16:775-84.
7. Hsiangfa L, Sungching C, Meichin C, Powei L, Chungtong C, Hsingwen S. Paclitaxel-loaded poly (γ -glutamic acid)-poly(lactide) nanoparticles as a targeted drug delivery system against cultured HepG2 cells. *Bioconjugate Chem.* 2006;17:291-9.
8. Shu-ichi S, Masahiro K, Hiroshi K, To-ru K. Complete regression of xenografted human carcinomas by a paclitaxel-carboxymethyl dextran conjugate (AZ10992). *J Control Release.* 2007;117:40-50.
9. Crosasso P, Ceruti M, Brusa P, Arpicco S, Dosio F, Cattel L. Preparation, characterization and properties of sterically stabilized paclitaxel-containing liposomes. *J Controlled Release.* 2000;63:19-30.
10. Hyukjin L, Kyuri L, Tae PG. Hyaluronic acid-paclitaxel conjugate micelles: synthesis, characterization, and antitumor activity. *Bioconjugate Chem.* 2008;19:1319-25.
11. Tarr BD, Sambandan TG, Yalkowsky SH. A new parenteral emulsion for the administration of taxol. *Pharm Res.* 1987;4:162-5.
12. Bae KH, Lee Y, Park TG. Oil-encapsulating PEO-PPO-PEO shell crosslinked nanocapsules for target-specific delivery of paclitaxel. *Biomacromolecules.* 2007;8:650-6.
13. Maeda H, Seymour LW, Miyamoto Y. Conjugates of anticancer agents and polymers: advantages of macromolecular therapeutics *in vivo*. *Bioconjugate Chem.* 1992;3:351-62.
14. Jian Y, Fu-Qiang H, Yong ZD, Hong Y. Polymeric micelles with glycolipid-like structure and multiple hydrophobic domains for mediating molecular target delivery of paclitaxel. *Biomacromolecules.* 2007;8:2450-6.
15. Shuliang L, Belinda B, JoEllen W, Andre FP. Self-assembled poly (butadiene)-b-poly (ethylene oxide) polymersomes as paclitaxel carriers. *Biotechnol Prog.* 2007;23:278-85.
16. Hyun JL, Hye YN, Byung HL, Dae JK, Jai YK, Jong-sang P. A novel technique for loading of paclitaxel-PLGA nanoparticles onto ePTFE vascular grafts. *Biotechnol Prog.* 2007;23:693-7.
17. Hosseinkhani H, Hosseinkhani M, Khademhosseini A, Kobayashi H. Bone regeneration through controlled release of bone morphogenetic protein-2 from 3-D tissue engineered nano-scaffold. *J Controlled Release.* 2007;117:380-6.
18. Hosseinkhani H, Hosseinkhani M, Tian F, Kobayashi H, Tabata Y. Osteogenic differentiation of mesenchymal stem cells in self-assembled peptide-amphiphile nanofibers. *Biomaterials.* 2006;27:4079-86.
19. Hosseinkhani H, Hosseinkhani M, Tian F, Kobayashi H, Tabata Y. Ectopic bone formation in collagen sponge self-assembled peptide-amphiphile nanofibers hybrid scaffold in a perfusion culture bioreactor. *Biomaterials.* 2006;27:5089-98.
20. Hosseinkhani H, Hosseinkhani M, Khademhosseini A, Kobayashi H, Tabata Y. Enhanced angiogenesis through controlled release of basic fibroblast growth factor from peptide amphiphile for tissue regeneration. *Biomaterials.* 2006;27:5836-44.
21. Hosseinkhani H, Hosseinkhani M, Kobayashi H. Design of tissue-engineered nanoscaffold through self-assembly of peptide amphiphile. *J Bioact Compat Polym.* 2006;21:277-96.

22. Entwistle J, Hall CL, Turley EA. HA receptors: regulators of signalling to the cytoskeleton. *J Cell Biochem.* 1996;61:569–77.
23. Stern R. Association between cancer and “acid mucopolysaccharides”: an old concept comes of age, finally. *Semin Cancer Biol.* 2008;18:238–43.
24. Hua Q, Knudson CB, Knudson WJ. Internalization of hyaluronan by chondrocytes occurs via receptor-mediated endocytosis. *J Cell Sci.* 1993;106:365–75.
25. Day AJ, Prestwich GD. Hyaluronan-binding proteins: tying up the giant. *J Biol Chem.* 2002;277:4585–8.
26. Toole BP, Slomiany MG. Hyaluronan: a constitutive regulator of chemoresistance and malignancy in cancer cells. *Semin Cancer Biol.* 2008;18:244–50.
27. Coradini D, Pellizzaro C, Miglierini G, Daidone MG, Perbellini A. Hyaluronic acid as drug delivery for sodium butyrate: improvement of the anti-proliferative activity on a breast-cancer cell line. *Int J Cancer.* 1999;81:411–6.
28. Coradini D, Zorzet S, Rossin R, Scarlata I, Pellizzaro C, Turrin C, *et al.* Inhibition of hepatocellular carcinomas *in vitro* and hepatic metastases *in vivo* in mice by the histone deacetylase inhibitor HA-But. *Clin Cancer Res.* 2004;10:4822–30.
29. Speranza A, Pellizzaro C, Coradini D. Hyaluronic acid butyric esters in cancer therapy. *Anticancer Drug Des.* 2005;16:373–9.
30. Luo Y, Bernshaw NJ, Lu Z, Kopecek J, Prestwich GD. Targeted delivery of doxorubicin by HPMA copolymer-hyaluronan bioconjugates. *Pharm Res.* 2002;19:396–402.
31. Luo Y, Prestwich GD. Synthesis and selective cytotoxicity of a hyaluronic acid-antitumor bioconjugate. *Bioconjugate Chem.* 1999;10:755–63.
32. Luo Y, Ziebell MR, Prestwich GD. A hyaluronic acid-taxol antitumor bioconjugate targeted to cancer cells. *Biomacromolecules.* 2000;1:208–18.
33. Wang Y, Xin D, Liu K, Xiang J. Heparin-paclitaxel conjugates using mixed anhydride as intermediate: synthesis, influence of polymer structure on drug release, anticoagulant activity and *in vitro* efficiency. *Pharm Res.* 2009;26:785–93.
34. Coradini D, Pellizzaro C, Abolafio G, Bosco M, Scarlata I, Cantoni S, *et al.* Hyaluronic-acid butyric esters as promising antineoplastic agents in human lung carcinoma: A preclinical study. *Invest New Drug.* 2004;22:207–17.
35. Shu-ichi S, Masahiro K, Hiroshi K, To-ru K. Paclitaxel delivery systems: the use of amino acid linkers in the conjugation of paclitaxel with carboxymethyl-dextran to create prodrugs. *Biol Pharm Bull.* 2002;25:632–41.
36. Peniche C, Arguelles-Monal W, Davidenko N, Sastre R, Gallardo A, Roman J. Self-curing membranes of chitosan/PAA IPNs obtained by radical polymerization: preparation, characterization and interpolymer complexation. *Biomaterials.* 1999;20:1869–78.
37. Chun L, Dong-fang Y, Robert AN, Fernando CL, Clifton S, Nancy H, *et al.* Complete regression of well-established tumors using a novel water-soluble Poly(L-Glutamic acid)-paclitaxel conjugate. *Cancer Res.* 1998;58:2404–9.
38. Rosler A, Vandermeulen GWM, Klok HA. Advanced drug delivery devices via self-assembly of amphiphilic block copolymers. *Adv Drug Deliv Rev.* 2001;53:95–108.
39. Hosseinkhani H, Aoyama T, Yamamoto S, Ogawa O, Tabata Y. *In vitro* transfection of plasmid DNA by amine derivatives of gelatin accompanied with ultrasound irradiation. *Pharm Res.* 2002;19:1471–9.
40. Hosseinkhani H, Aoyama T, Ogawa O, Tabata Y. Tumor targeting of gene expression through metal-coordinated conjugation with dextran. *J Controlled Release.* 2003;88:297–312.
41. Hosseinkhani H, Tabata Y. PEGylation enhances tumor targeting of plasmid DNA by an artificial cationized protein with repeated RGD sequences, Pronectin. *J Controlled Release.* 2004;97:157–71.
42. Hosseinkhani H, Azzam T, Tabata Y, Domb AJ. Dextran-spermine polycation: an efficient nonviral vector for *in vitro* and *in vivo* gene transfection. *Gene Ther.* 2004;11:194–203.
43. Hosseinkhani H, Tabata Y. Ultrasound enhances *in vivo* tumor expression of plasmid DNA by PEG-introduced cationized dextran. *J Controlled Release.* 2005;108:540–56.
44. Nicolaou KC, Rlemer C, Kerr MA, Rideout D, Wrasidlo E. Design, synthesis and biological activity of protaxols. *Nature.* 1993;364:464–6.
45. Schiff PB, Horwitz SB. Taxol stabilizes microtubules in mouse fibroblast cells. *Proc Natl Acad Sci.* 1980;77:1561–5.
46. Jordan MA, Wendll K, Gardiner S, Derry WB, Copp H, Wilson L. Mitotic block induced in HeLa cells by low concentrations of paclitaxel (Taxol) results in abnormal mitotic exit and apoptotic cell death. *Cancer Res.* 1996;56:816–25.

Reproduced with permission of the copyright owner. Further reproduction prohibited without permission.